Magnetoresistive Sensors with Rapidly Solidified Permalloy Fibers

P. Ciureanu, G. Rudkowska, P. Rudkowski, and J. O. Ström-Olsen

Abstract—**The microstructure of Permalloy fibers shows columns growing perpendicular to the contact line between the melt and the extraction wheel. Strong tensile stresses are believed to develop along the columns and are incorporated in the fiber during solidification. As a result, the easy axis of magnetization of fibers is perpendicular to their length. Both transverse and longitudinal extraordinary magnetoresistive effects have a positive initial slope due to stress-related rotation of moments in the closure domains and to the coherent rotation of moments in the columns. Fiber response was also investigated as a function of the field direction and angle of incidence, fiber twisting and for strong transverse fields. The results are discussed in terms of the existing models. The longitudinal effect is analyzed in terms of the Jones–Soohoo model, whereas a new model is proposed to explain the transverse effect. Both effects are useful for sensing purposes, but we have been used only the longitudinal effect for our sensors. The structures and operating principles of single- and dual-fiber biased sensors are presented in detail. Distortions due to overbiasing are accounted for the pinning and expansion of large-area closure domains with moments tilted by the casting stress. The sensitivity–linearity range product is the same for several bias levels and a family of sensors was obtained using the same fiber. The performances of the fiber sensors are compared to those of thin-film sensors. Noise, self-heating, encasing and manufacturing are also discussed and optimistic conclusions are found for fiber sensors.**

I. Introduction

SOFT magnetic materials are widely used in sensors which measure or detect magnetic fields. The sensing element is usually a thin-film magnetoresistor made of a zero-magnetostriction ferromagnetic alloy (NiFe or NiFeCo). Recently, such materials have been produced in a fiber form by using a rapid solidification method. Investigation of these fibers have shown them to be very suitable as magnetoresistive sensors. In fact, the sensitivity of NiFe fibers was found to be similar to that of thin NiFe films. These fibers have also a small enough diameter in order to exhibit quite high resistance and output signal.

II. Casting and Structure of Fibers

The casting method has been described in greater detail earlier [1], [2]. A ferromagnetic rod made of an 81% wt Ni 19% wt Fe alloy is melted at the tip and the fibers were extracted from the melt by a rapidly rotating sharpened molybdenum wheel. The process took place under helium gas to inhibit oxidation. The average diameter of fibers was about 15 μm [3] and the resistivity of the material 40 $\mu\Omega$cm, larger than the resistivities of both bulk 81Ni19Fe alloy (15 $\mu\Omega$cm) and thin 81Ni19Fe films (25 $\mu\Omega$cm). The average cross-sectional area of the fiber is about 200 μm^2 and is much larger than the typical value of thin film magnetoresistors (5 μm^2).

Fig. 1. SEM micrograph of a NiFe fiber showing the contact line.

Fiber samples were examined by scanning electron microscopy (JEOL T300). The surface of the fiber was initially etched using a 1 : 1 mixture of nitric acid and glacial acetic acid in order to reveal the columns which grow away from the contact line between the melt and the rotating wheel (see Fig. 1). The columns are clearly perpendicular to the contact line of the fiber. The transverse cross-section of the fibers is quasi-circular in shape and the directions of columns growth converge to a point at the contact line. The temperature gradients during solidification are directed from the contact point towards the fiber surface, which is the last to solidify. We assume that strong tensile stresses, showed by double arrows in Fig. 2, develop along the columns. In fact, the material is removed from the liquid phase and expands away from the edge of the rotating wheel in a radial direction. The rapid solidification prevents any elastic counteraction which can relax the strain, leading to strong quenched-in tensile stresses.

Manuscript received October 29, 1992; revised February 9, 1993.

The authors are with the Physics Department, McGill University Centre for the Physics of Materials, 3600 University, Montreal, Quebec, Canada, H3A 2T8.

IEEE Log Number 9209603.

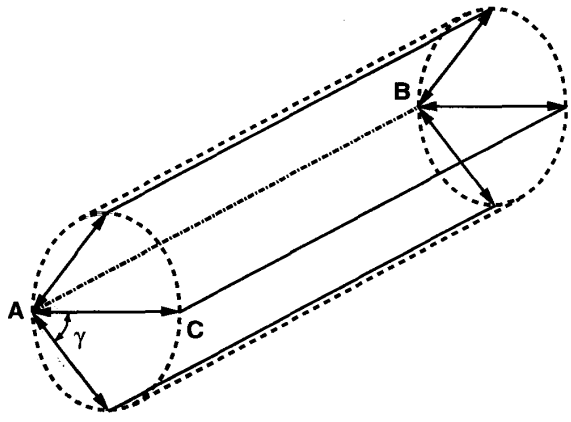

Fig. 2. Structure of the NiFe fiber showing three column directions (γ = 0 and $\pm\pi/4$) and the corresponding longitudinal cross-sectional planes. AB is the contact line and AC is the main column direction (γ = 0).

A model of the magnetic structure of the fiber is proposed in Fig. 2. The melt extraction determines uniaxial anisotropies in all planes which contain the contact line and the direction of a column, with easy axes of magnetization parallel to the stress direction [4]. The casting anisotropy seems to be much stronger than the shape anisotropy and so the easy axis remains perpendicular to the fiber length. The fiber may be viewed in our model as an assembly of thin films with in-plane uniaxial anisotropy, fanning around the contact line (Fig. 2). The magnetoresistive response of the fiber is then the superposition of the responses of all these planes. This model is consistent with the results to be presented below.

III. Magnetoresistive Responses

As-cast NiFe fibers were placed in the center of a pair of Helmholtz coils and quadratic extraordinary magnetoresistive effects were found to develop in the presence of a magnetic field. The fiber was supplied with a 20 mA constant current and the voltage drop across the fiber ranged between 200 and 800 mV, depending on the fiber length and diameter. The variations in the voltage drop were measured by a differential microvoltmeter (John Fluke 887A) after the fiber reached thermal equilibrium. In fact, Permalloy fibers are very sensitive to temperature changes. For this purpose, the fiber was kept during measurements inside a hermetically closed plexiglass box or was embedded in an epoxy resin. About 10 min of self-heating were found to be enough to reach a thermal equilibrium at a 20 mA sensing current. We estimate the temperature increases by less than ten degrees above the room temperature (Joule self-heating data will be provided in Section VIII). The testing set is shown in the inset in Fig. 4. The magnetoresistive response is defined as the ratio of the difference between the fiber resistivity, resistance or voltage drop at a given magnetic field and in zero field to the same values in zero field, i.e.: $\Delta U/U = [U(H) - U(H = 0)]/U(H = 0)$. The longitudinal magnetoresistive response $\Delta U_l/U$ was measured with the field applied parallel to the fiber, whereas the transverse response $\Delta U_t/U$ was measured with the field perpendicular to the fiber. The longitudinal effect was stronger (up to 3%) than the transverse one (about 1%) and the slope of the response in the small-field domain was much larger for the longitudinal effect (see Fig. 3). Both effects are positive, in contrast to the behavior in thin NiFe films [5]. However, a similar behavior was observed in FeSiB amorphous wires, where both effects showed initially a negative slope [6].

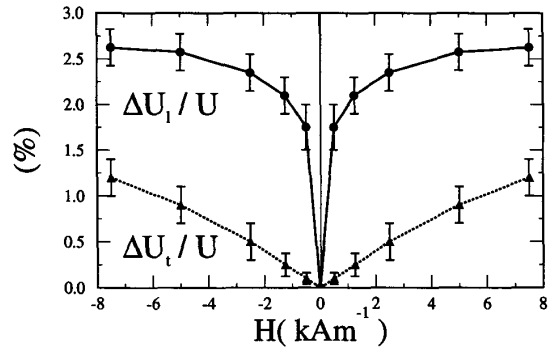

Fig. 3. Longitudinal and transverse magnetoresistive responses of NiFe fibers.

The magnetoresistive response of NiFe fibers was also plotted as a function of the magnetic field direction. A 7.5 kAm^{-1}-strong field was applied by the Helmholtz coils and the fiber was rotated horizontally by an angle α between the coils (see Fig. 4). The data in Figs. 3 and 4 are in good agreement and the 1% minimum and 3% maximum positive effects are found again when the fiber is perpendicular and, respectively, parallel to the field direction.

The transverse response of the fiber was further investigated as a function of the angle of incidence of the applied field. The fiber was placed perpendicular to the 7.5 kAm^{-1} field direction and then rotated around its axis by an angle β. A periodic function was obtained, with maxima at 0 and 180 degrees and minima at β = 90 degrees (see Figure 5). This behavior can be explained by taking into account the "palmar" structure of the fiber in transverse cross-section. Actually, the fiber was placed onto the substrate with the contact line lying in the left horizontal side, which corresponds to β = 0. The transverse effect should be proportional to the field strength and the amount of material involved in the magnetization process.

As we shall see in the next section, the transverse variation in resistivity may be explained by the rotation of moments in the closure domains towards the current path. The higher the components of the transverse field along columns are, the larger the effect is. So, for β = 0 the interaction between the applied field and the moments in the closure domains reaches a maximum. This interaction drops to a minimum for β = 90 degrees when the field becomes perpendicular to the main column and does not rotate its moments with respect to the current path.

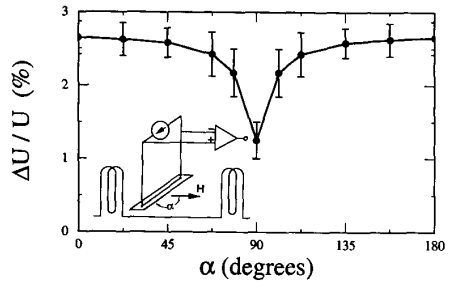

Fig. 4. Magnetoresistive response of NiFe fibers versus field direction.

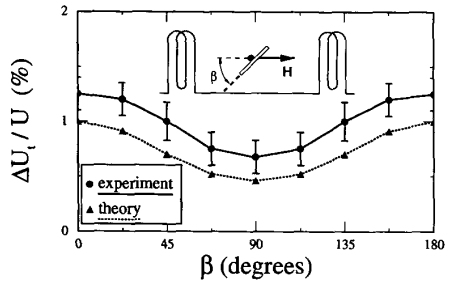

Fig. 5. Transverse magnetoresistive response of NiFe fibers versus angle of incidence of the applied field.

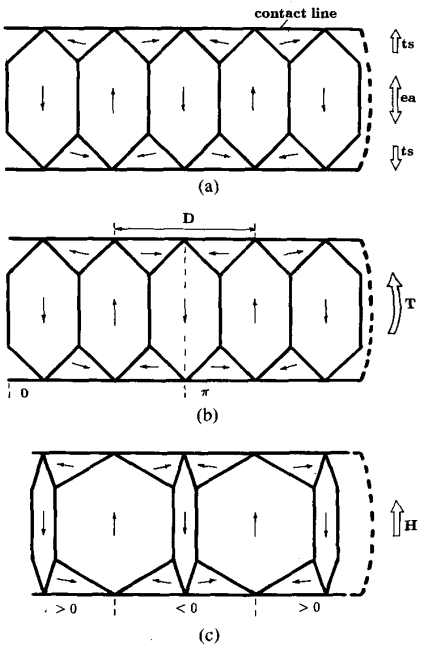

Fig. 6. The transverse magnetization process of NiFe fibers: (a) as-cast specimen; (b) fiber twisted by π; (c) twisted fiber in small transverse field.

The contribution of the other columns decreases proportionally to their length due to the smaller area occupied by the closure domains and then the smaller amount of material interacting with the transverse field. From simple geometric considerations and superposition theorem, the transverse response for a given β may be written as

$$\Delta U_t/U \sim \sum_{\gamma=-\pi/4}^{\pi/4} \cos\gamma\,|\cos(\beta-\gamma)| \qquad (1)$$

where β is the angle defined in Fig. 5 and γ the angle defined in Fig. 2. The modulus in (1) stands for the symmetry in the transverse magnetization of fibers, as we shall see below. Only five columns have been considered (γ = 0, ± 22.5 and ± 45 degrees). The relative length of each column was multiplied by the relative strength of the field along that column and the results for a given angle of incidence have been added. The theoretical response was first normalized to its maximum value and then plotted in Fig. 5. A good agreement between theory and experiment was obtained, which strongly endorses our model of the magnetic structure of the fiber.

IV. The Transverse Magnetization of Fibers

The initial positive slope of the transverse effect of NiFe fibers can be explained only by taking into account the tensile stresses directed along the columns and incorporated during fiber solidification. It is known that the magnetic moments can also be rotated by applying a stress, rather than a magnetic field. This anisotropic change in resistivity was called "elasto-magnetoresistance" by Restorff *et al.* [7]. Any of the planes depicted in Fig. 2 will show the moments in the closure domains slightly rotated towards the stress directions (see Fig. 6(a) where the thin arrows are the magnetic moments, *ts* are the tensile stress directions and *ea* is the easy axis). If a transverse field of up to 7.5 kAm^{-1} is applied to the fiber, an increase in resistivity will occur when the moments in the closure domains will rotate towards the current path (the length of the fiber). Several assumptions are made to explain this behavior.

1) The tensile stresses incorporated in the fiber during solidification slightly rotate the moments in the closure domains away from the current path.

2) The tensile stress can be released by twisting the fiber.

3) A 7.5 kAm^{-1} transverse field can rotate the moments in the closure domains only by very small angles. Higher field is necessary to align the moments to the current path and a much higher field is required to rotate these moments perpendicular to the current path.

The first assumption was derived from known phenomena in ferromagnetic bodies. The second assumption was verified experimentally by placing the fiber in a 7.5 kAm^{-1} transverse field and by twisting one end or both ends in opposite directions. The transverse effect versus the number of twists was found to be a periodic function with monotonic decrease in the average value. The period was one rotation for single twisting (see Fig. 7) and half rotation for double twisting, and maxima and minima of the functions succeeded in both cases after an π relative rotation between the fiber's ends. The transverse effect progressively disappeared as the incorporated stress was released due to the twisting. On the other hand, the lon-

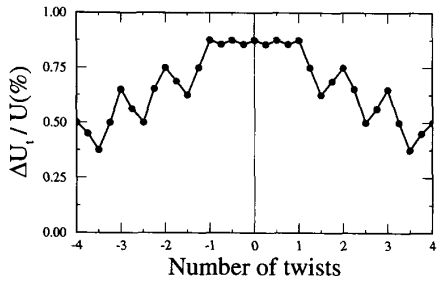

Fig. 7. Transverse response of a single twisted NiFe fiber versus the number of twists.

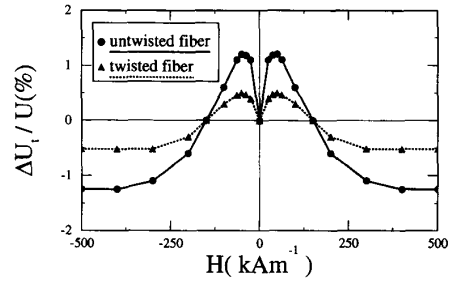

Fig. 8. The magnetoresistive response of NiFe fibers in high transverse field.

gitudinal effect remained unchanged after the fiber twisting.

The third assumption was verified also by a simple experiment. An electromagnet provided the fiber with a transverse field of up to 800 kAm^{-1}. A positive maximum in the transverse effect occurred around 50 kAm^{-1} and was followed by a zero-crossing at 150 kAm^{-1} and then by a negative saturation at about 500 kAm^{-1} (see Fig. 8). The maximum negative effect ranged between the positive maximum effect and twice this value. The transverse effect of twisted fibers was smaller than that of untwisted ones and the position of maxima was preserved. So, very high fields are required to counteract the strong edge demagnetization of the fiber.

Using these assumptions, a new model to explain the transverse magnetoresistive effect of NiFe fibers is proposed (see Fig. 6(a)). We attribute the increase in the fiber resistivity for small upwards transverse fields to the slight rotation of moments in the bottom closure domains towards the current path. On the other hand, the moments in the top closure domains cannot be further rotated away from the current path, according to assumption no. 3. For downwards fields, only the moments in the top closure domains are allowed to rotate towards the current path. Twisting the fiber was found to annihilate the transverse effect. This can be explained by considering a torsion moment T which twists by π the right half of the fiber segment in Fig. 6(b). A torsion stress appears in the transverse cross-section which separates the two halves of the segment, so that the local stress is released over the region D. The moments in the closure domains become parallel to the edges of the fiber in this stress-free region. When a small upwards field H is applied, these moments will rotate slightly away from the current path and the resistivity of the fiber will decrease. The resisitivity still increases in all the other regions due to the small rotation of moments towards the current path in the bottom domains (see Fig. 6(c) where <0 and >0 denote the signs of the transverse effect). With further twisting, the stress-free regions will expand at the expense of initially stressed regions and the transverse effect of the fiber will cancel out.

The transverse magnetization of the fiber takes place along the easy axis direction and the magnetization process consists of the wall displacement of main domains, which does not affect the resistivity, accompanied by a small-angle rotation of moments in the closure domains, which affects the resistivity. A quite large transverse effect was found (about 1/3 of the longitudinal one); this is due to the large amount of material occupied by the closure domains, whose moments interact with the applied field. The transverse effect is positive at low fields and can be annihilated or reversed by twisting the fiber or by subjecting it to a very strong field.

V. The Longitudinal Magnetization of Fibers

The longitudinal magnetoresistive effect in Permalloy fibers can be quite accurately explained by the Jones–Soohoo model of magnetization of a long NiFe strip with the easy axis perpendicular to the strip's length [8], [9], [10]. The domain pattern in any of the longitudinal planes which form the fiber is similar to that of a hard-axis driven thin film. The longitudinal magnetization of the fiber should then occur through coherent rotation of moments in the main domains generated in the columns, accompanied by the wall displacement of the closure domains pinned at the fiber's edges. The longitudinal effect is positive and causes an increase in the fiber resistivity when the moments in the main domains rotate towards the current path (the length of the fiber).

A modified Jones–Soohoo model should be considered for NiFe fibers, where the closure domains also account for the longitudinal magnetoresistive response of fibers. In fact, the moments in these domains are slightly rotated away from the current path by the tensile stresses (see Fig. 9(a)). When an up to 7.5 kAm^{-1} longitudinal field is applied, the 90 degrees walls of closure domains begin to move forming new angles, as shown in Fig. 9(b), where θ is the rotation angle in the main domains, denoted by 1, 3, 5, and 7. Closure domains no. 2, 4, and 6 with the moments directed towards the field H strongly expand and their moments slightly rotate, whereas closure domains with opposite orientation disappear. For a H_s = 7.5 kAm^{-1} saturating longitudinal field, at which the moments in the main domains align to the field direction, the moments in the closure domains are still tilted, accordingly to assumption no. 3 in Section IV (see Fig. 9(c)). This fact has as a consequence the distortion of the longitudinal response of the biased fiber sensor at high biasing levels, as we will see soon. This distortion always occurs for sensing fields which have the same polarity as the bias field has. Pinning and expansion of large-area closure domains, which occupy much of the fiber and in-

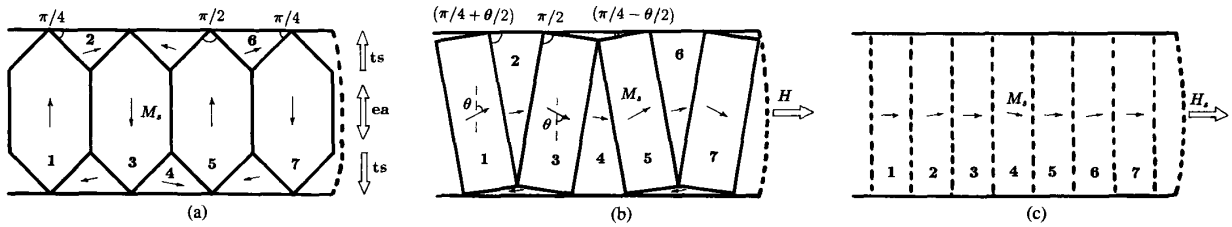

Fig. 9. The longitudinal magnetization process of NiFe fibers: (a) as-cast specimen; (b) fiber in small longitudinal field; (c) fiber in saturating longitudinal field.

teract with the applied field, could explain the distorted behavior of these sensors.

The longitudinal magnetization of the fiber takes place along the hard axis direction and the magnetization process consists of the coherent rotation of moments in the main domains, accompanied by a small angle rotation of moments in the closure domains, which both affect the resistivity, and by the wall displacement of the closure domains, which does not affect the resistivity. The longitudinal magnetoresistive effect is the useful effect for sensing purposes due to its large magnitude and the ease of fiber biasing. Pinning of large closure domains with tilted moments by high bias fields produce response distortion for sensing fields with the same polarity as the biasing ones.

VI. The Single-Fiber Biased Sensor

As-cast NiFe fibers 15 μm in diameter (average cross-sectional area of 200 μm^2) and 1 cm-long have a resistance in zero magnetic field of about 20 Ω and represent sensitive unbiased sensors, very suitable for position detection or contactless control purposes. To detect the polarity of the sensing field, the sensor must be linearized by applying a bias field parallel to the length of the fiber. The single-fiber based sensor consists of a Permalloy fiber passing through a ceramic tube 1 cm-long and 1 mm in external diameter. The ends of the fiber are connected to a 20 mA-constant current source, on one hand, and to a differential microvoltmeter, on the other hand (see Fig. 10). The sensing field H must be applied along the fiber. An 150–200-turn coil, made of copper insulated wire 0.15 mm in diameter, is wound around the tube. A constant current flows through the coil and provides the fiber with a H_b bias field. This field superposes with the sensing field and shifts the operating point $H = 0$ of the sensor from the peak to the linear region of the response (see Figure 11).

The magnitude of the biasing is given by the MMF of the coil (amps.turns or AT). By reversing the direction of H_b the response symmetrically shifts towards positive fields. The negative biased characteristics in Fig. 11 show that at low bias levels (around 2.5 AT), linear responses through the origin are obtained. The sensor sensitivity is defined as the ratio of the voltage drop change to the linearity range of the sensor ($\Delta U/\Delta H$) and represents the slope of the linear region of the response which passes through the origin. A sensitivity of about 8μV A^{-1}m was obtained for a 20 mA sensing current and a fiber resistance of 20Ω. At higher bias levels (5 AT) the sensitivity drops to 4 μV A^{-1}m, but the range of linearity in detecting magnetic fields increases from ±250 $Am^{-1}$to ±500 Am^{-1}. The sensitivity–linearity range product is the same in the two cases, which reflects the response distortion occurring at higher bias. In fact, the response at 2.5 AT bias has smaller amplitude and larger negative pulse width than the response of unbiased sensor. This behavior is more evident at 5 AT bias, where a slight nonlinearity of the response may be also noticed. Over 12 AT bias, the sensor operates in a highly nonlinear regime.

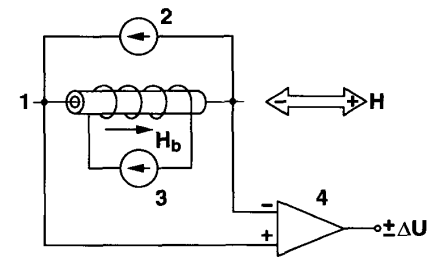

Fig. 10. The single-fiber biased sensor: 1) NiFe fiber. 2) Sensing current source. 3) biasing current source. 4) Differential microvoltmeter.

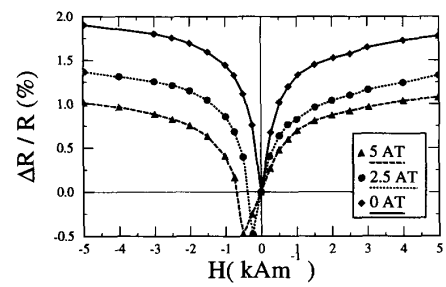

Fig. 11. Magnetoresistive responses of the single-fiber sensor for three bias levels.

When dc measurement was used to plot the sensor response, thermal drift due to the sensor and electronics was added to the response and frequent zero adjustment was necessary during the measurement. The thermal drift due to electronics was cancelled out by using a four-wire ac resistance bridge (Linear Research LR-400) to plot the responses in Fig. 11. The sensing current was 1 mA in amplitude and 15.9 Hz in frequency. The difference between the fiber resistance and a pre-set resistance (the fiber resistance in zero magnetic field) was available at the output of a tuned amplifier. The ac response was found to be identical to the dc response, after the fiber reached thermal equilibrium. The thermal drift due to the sensor

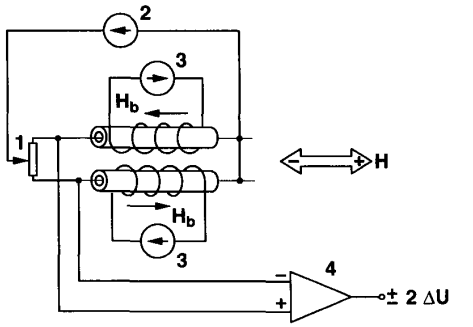

Fig. 12. The dual-fiber biased sensor: 1-potentiometer; 2-sensing current source; 3-biasing current source; 4-differential microvoltmeter.

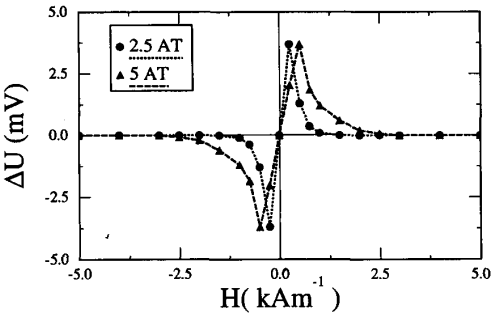

Fig. 13. Magnetoresistive responses of the dual-fiber sensor for two bias levels.

can be cancelled out only for dual-fiber sensors arranged in a Wheatstone bridge circuit.

VII. The Dual-Fiber Biased Sensor

This sensor consists of two single-fiber biased sensors, arranged so as to form two active arms of a Wheatstone bridge (see Fig. 12). The passive arms of the bridge are formed by the two halves of a 50Ω potentiometer. The sensing currents are provided by a 40 mA constant current source and run in parallel through the fibers. Separate bias current sources are used in such a way that equal in magnitude but opposite in direction bias fields are provided to the fibers. The output signal is picked-up from the diagonal of the bridge and $\pm 2\ \Delta U$ is measured by the differential microvoltmeter. Actually, for a given sensing field, the resistivity of one fiber increases whereas that of the other one decreases due to the antisymmetric bias. The dual sensor sensitivity is then twice the sensitivity of the single sensor. The thermal drift is also cancelled out when the temperature in the sensor area changes. In fact, the operating points of the two fibers are shifted in the same direction on to the individual responses, giving a zero drift in the differential output.

Fig. 13 shows the magnetoresistive responses of the dual sensor for two bias levels. The dc measurement was used again and the differential microvoltmeter was used as a null instrument. The bridge was balanced before plotting each curve by readjusting the potentiometer. No zero drift was observed and the increase in sensitivity was obvious (16 μV A^{-1}m at 2.5 AT bias and 8 μV A^{-1}m at 5 AT bias).

The output signal of the dual sensor was observed using an oscilloscope which replaced the microvoltmeter in the bridge. The sensor was placed between the Helmholtz coils which were driven by an 100 Hz sinewave current. A multimeter was used to monitor the strength of the current through these coils. An 8 mV_{pp} sinusoidal voltage was observed on the screen for bias levels up to 8 AT and maximum fields at which the sinusoid was undistorted. Linear field ranges of about ± 800, ± 500 and ± 250 Am^{-1} were observed for bias levels of 8, 5 and, respectively, 2.5 AT. If the bias current is larger than its optimum strength, a decrease in output amplitude will occur. On the contrary, peak distortion appears in the sinusoid when the bias level is lower than its optimum value.

VIII. Comparison with Existing Devices

The only existing devices on the market are thin-film magnetoresistors, classified in Table I according to their biasing method. This table lists the main performances of thin-film sensors, compared with those of fiber sensors. It is obvious that, for the same magnetoresistive effect of the material, the output signal and then the sensitivity are larger for higher resistance sensors. However, the 4 mV_{pp} output signal of the single fiber sensor is well above the noise induced by the fiber and the measuring circuit. An important feature of the fiber sensor is that a family of devices, with different sensitivities and linearity ranges, can be obtained with the same fiber by varying the biasing level. This is more convenient than for thin-film magnetoresistors, where the shape of the layer must be changed in order to modify their performances.

The noise of the dual fiber sensor was measured by replacing the sensing current generator in the Wheatstone bridge with a 1.5 V battery. The sensing current through the fibers increased to 33 mA and was totally noise-free. A 13 mV_{pp} sinewave signal was then picked-up from the bridge and displayed on the oscilloscope. The Helmholtz coils were supplied with a 100 Hz sinewave current and the amplitude of the measured magnetic field was of about 1 kAm_{pp}^{-1} for a 5 AT bias level of the sensor. No distortion of the output sinusoid was observed. Then the sensing field was cut-off and a noise of about 100 μV_{pp} was observed on the screen. The oscilloscope filter was set to $HF = 3$ MHz for this measurement. An 40 dB signal-to-noise ratio was found for our dual fiber sensor, a typical value for thin-film magnetoresistors [11].

The size of the sensor is very important in this miniaturization era. The canted easy axis magnetometer in Table I, for example, is a large-area sensor with a very long sensing path [12], which explains the high values of both sensitivity and output signal. Barber-pole magnetometers [13] are miniature sensors with an active sensing area of 1.6×1.6 mm^2. The "insulated" shunt dual sensor [14] had an active area of 1×0.05 mm^2. But the size of a solid-state device is mainly determined by the area of the connecting pads. So, the volume occupied by a thin-film magnetoresistor can easily reach $2 \times 5 \times 5$ mm^3. Our dual fiber sensor was encased in a cylinder 5 mm in diameter and 1 cm long. The single sensor is even slimmer and the unbiased sensor may be viewed as a microsensor.

TABLE I
COMPARISON OF DEVICES

Sensor	Sensitivity ($\mu V\ A^{-1}\ m$)	Linear field range (kAM^{-1})	Sensor resistance (Ω)	Max. output signal (mV)	Reference
Canted-easy-axis magnetometer	100	±0.2	4300	±20	[12]
KMZ10A barber-pole magnetometer	20	±1	250	±20	[13]
"Insulated"-shunt dual sensor	8	±1	160	±8	[14]
Single-fiber	4	±0.5	20	±2	—
biased sensor	8	±0.25			
Dual-fiber	8	±0.5	20	±4	—
biased sensor	16	±0.25			

No noticeable self-heating of the fibers was observed during the measurements. The current density in the fiber was about 0.1 mA $(\mu m)^{-2}$, ten times lower than the usual current density in thin NiFe film magnetoresistors. The Joule self-heating of the fiber is about 10 mW. On the other side, fiber sensors do not have a substrate to act as a heat sink, as thin film sensors do, and the resistivity of the material is somewhat higher in fibers. Self-heating of the coils is also negligible due to the small bias current required for an efficient bias (10^{-3} mA $(\mu m)^{-2}$), in strong contrast with "insulated"-shunt biased sensors which require a bias current density as high as 1 mA $(\mu m)^{-2}$. However, the rise in temperature of latter sensors was only about 10°C above room temperature [5]. We may conclude that the thermal regime of fiber sensors encased in epoxy resine is better than that of a multi-layered thin film sensor. The residual thermal drift of dual sensors can be compensated by thermistors included in the bridge or by electronic means.

The Permalloy fibers are produced in one manufacturing step only, which does not require sophisticated and costly sputtering plants, aligning machines or clean rooms, as thin-film sensors do. The fiber sensor does not need any substrate or special connecting pads. The measuring circuitry is the same as for conventional magnetoresistors and the applications of the fiber sensors are mainly the same as those of thin-film sensors. But the fabrication technology seems to be easier to implement and the price/performance ratio should be much lower.

IX. Conclusions

Permalloy fibers have been proved to be very suitable as sensing elements for magnetoresistive devices. The fiber sensitivity is of the same order of magnitude as the sensitivity of thin-film magnetoresistors. A simple biasing technique was used to linearize the sensor operation. The stress incorporated in the fiber during solidification strongly influences the magnetization process and the slope of the linearized response changes as a function of the bias level. A versatile sensor was then obtained using the same fiber, but a compromise between sensitivity and linearity range should be reached for any particular application.

Acknowledgment

Professor Arthur Yelon from Ecole Polytechnique de Montreal kindly helped us to understand the magnetization processes occurring in the fiber.

References

[1] P. Rudkowski and J. O. Ström-Olsen, U.S. Patent 5,003,291 March 26, 1991.
[2] P. Rudkowski, G. Rudkowska, J. O. Ström-Olsen, C. Zeller, and R. Cordery, "The magnetic properties of sub-20-μm metallic fibers formed by continuous melt-extraction," *J. Appl. Phys.*, vol. 69, no. 8, part II A, pp. 5017–5019, 1991.
[3] P. Rudkowski, G. Rudkowska, A. Zaluska, and J. O. Ström-Olsen, "The properties of sub-20-μm Permalloy fiber formed by melt extraction," *IEEE Trans. Magn.*, vol. 28, no. 4, pp. 1899–1903, 1992.
[4] A Siemko, H. K. Lachowitz, N. Moser, A. Forkl, and H. Kronmüler, "Stress-anneal-induced anisotropy in metallic glasses," *J. Magn. Magn. Mater.*, vol. 83, pp. 171–173, 1990.
[5] P. Ciureanu, *Magnetoresistive Sensors* in P. Ciureanu and S. Middelhoek (eds.) *Thin Film Resistive Sensors* (IOP Publishing: Bristol) 495 pages, 1992.
[6] Y. Makino, J. L. Costa, V. Madurga, and K. V. Rao, "Magnetoresistance, stress effects and a self-similar expansion model for the magnetization process in amorphous wires," *IEEE Trans. Magn.*, vol. MAG-25, no. 5, pp. 3620–3622, 1989.
[7] J. B. Restorff, M. Wun-Fogle, K. B. Hathaway, and A. E. Clark, "Anisotropic magnetoresistance in magnetorestrictive Metglas 2605SC for strain gage applications," *J. Appl. Phys.*, vol. 69, no. 8, pp. 4668–4670, 1991.
[8] R. E. Jones, Jr., "Domain effects in the thin film head," *IEEE Trans. Magn.*, vol. MAG-15, no. 6, pp. 1619–1621, 1979.
[9] R. F. Soohoo, "Switching dynamics in a thin film recording head," *IEEE Trans. Magn.*, vol. MAG-18, no. 6, pp. 1128–1130, 1982.
[10] R. F. Soohoo, "Magnetization processes in a thin film recording head," *J. Appl. Phys.*, vol. 57, no. 1, pp. 3949–3951, 1985.
[11] N. Smith, F. Jeffers, and J. Freeman, "A high-sensitivity magnetoresistive magnetometer," *J. Appl. Phys.*, vol. 69, no. 8, pp. 5082–5084, 1991.
[12] W. Kwiatkowski and S. Tumanski, "Permalloy magnetoresistive sensors. Properties and applications," *J. Phys. E: Sci. Instrum.*, vol. 19, no. 7, pp. 502–515, 1986.
[13] Valvo-Philips G.m.b.H., "D.c. magnetometer" Technical Publication no. 102, 1983.
[14] P. Ciureanu and G. Korony, "Effects of annealing and geometry optimization on a thin magnetoresistive head," *Sensors and Actuators*, vol. 13, pp. 229–241, 1988.

P. Ciureanu biography not available at time of publication.

G. Rudkowska biography not available at time of publication.

P. Rudkowski biography not available at time of publication.

J. O. Ström-Olsen biography not available at time of publication.